

A Novel Multiple-kernel based Fuzzy c-means Algorithm with Spatial Information for Medical Image Segmentation

Nookala Venu

Research Scholar

Department of Electronics and Communication Engineering

Sri Venkateswara University College of Engineering

Sri Venkateswara University, Tirupati-517502, India

venunookala@gmail.com

Dr. B. Anuradha

Professor

Department of Electronics and Communication Engineering

Sri Venkateswara University College of Engineering

Sri Venkateswara University, Tirupati-517502, India

anubhuma@yahoo.com

Abstract

Fuzzy c-means (FCM) algorithm has proved its effectiveness for image segmentation. However, still it lacks in getting robustness to noise and outliers, especially in the absence of prior knowledge of the noise. To overcome this problem, a generalized a novel multiple-kernel fuzzy c-means (FCM) (NMKFCM) methodology with spatial information is introduced as a framework for image-segmentation problem. The algorithm utilizes the spatial neighborhood membership values in the standard kernels are used in the kernel FCM (KFCM) algorithm and modifies the membership weighting of each cluster. The proposed NMKFCM algorithm provides a new flexibility to utilize different pixel information in image-segmentation problem. The proposed algorithm is applied to brain MRI which degraded by Gaussian noise and Salt-Pepper noise. The proposed algorithm performs more robust to noise than other existing image segmentation algorithms from FCM family.

Keywords: FCM, Image Segmentation, Gaussian Kernal, Fuzzy, Multiple-Kernal.

1. INTRODUCTION

Image segmentation is one of the first and most important tasks in image analysis and computer vision. In the literature, various methods have been proposed for object segmentation and feature extraction, described in [1] and [2]. However, the design of robust and efficient segmentation algorithms is still a very challenging research topic, due to the variety and complexity of images. Image segmentation is defined as the partitioning of an image into non overlapped, consistent regions which are homogeneous in respect to some characteristics such as intensity, color, tone, texture, etc. The image segmentation can be divided into four categories: thresholding, clustering, edge detection and region extraction. In this report, a clustering method for image segmentation will be considered.

The application of image processing techniques has rapidly increased in recent years. Nowadays, capturing and storing of medical images are done digitally. Image segmentation is to partition image to different regions based on given criteria for future process. Medical image segmentation is a key task in many medical applications. There are lots of methods for automatic and semi automatic image segmentation, though, most of them fail in unknown noise, poor image contrast, and weak boundaries that are usual in medical images. Medical images mostly contain complicated structures and their precise segmentation is necessary for clinical diagnosis [3].

Magnetic resonance imaging (MRI) is a very popular medical imaging technique, mainly because of its high resolution and contrast, which represent great advantage above other diagnostic imaging modalities. Besides all these good properties, MRI also suffers from three Considerable obstacles: noises (mixture of Gaussian and impulse noises), artifacts, and intensity in homogeneity [4].

In recent literatures, several approaches are there for medical image segmentation. The available segmentation methods in literature for medical images are: thresholding approaches, clustering approaches, classifiers, region growing approaches, Artificial Neural Networks (ANNs), deformable models; Markov Random Field (MRF) models atlas-guided approaches and so on. Amongst the above said methods, in medical imaging research clustering based approaches perceived a great focus of interest.

Clustering is a process for classifying objects or patterns in such a way that samples of the same cluster are more similar to one another than samples belonging to different clusters. There are two main clustering strategies: the hard clustering scheme and the fuzzy clustering scheme. Forgy and MacQueen [5] proposed K-means clustering algorithm. K-means is one of the hard clustering method. The conventional hard clustering methods classify each point of the data set just to one cluster. As a consequence, the results are often very crisp, i.e., in image clustering each pixel of the image belongs just to one cluster. However, in many real situations, issues such as limited spatial resolution, poor contrast, overlapping intensities, noise and intensity in homogeneities reduce the effectiveness of hard (crisp) clustering methods. Fuzzy set theory [7] has introduced the idea of partial membership, described by a membership function. Fuzzy clustering, as a soft segmentation method, has been widely studied and successfully applied in image clustering and segmentation [8]–[13]. Among the fuzzy clustering methods, fuzzy c-means (FCM) algorithm [14] is the most popular method used in image segmentation because it has robust characteristics for ambiguity and can retain much more information than hard segmentation methods [15]. Although the conventional FCM algorithm works well on most noise-free images, it is very sensitive to noise and other imaging artifacts, since it does not consider any information about spatial context.

To compensate this drawback of FCM, a pre-processing image smoothing step has been proposed in [13], [16], and [17]. However, by using smoothing filters important image details can be lost, especially boundaries or edges. Moreover, there is no way to control the trade-off between smoothing and clustering. Thus, many researchers have incorporated local spatial information into the original FCM algorithm to improve the performance of image segmentation [9], [15], [18].

Tolias and Panas [9] developed a fuzzy rule-based scheme called the ruled-based neighborhood enhancement system to impose spatial constraints by post processing the FCM clustering results. Noordam et al. [10] proposed a geometrically guided FCM (GG-FCM) algorithm, a semi-supervised FCM technique, where a geometrical condition is used determined by taking into account the local neighborhood of each pixel.

Pham [19] modified the FCM objective function by including spatial penalty on the membership functions. The penalty term leads to an iterative algorithm, which is very similar to the original FCM and allows the estimation of spatially smooth membership functions.

Ahmed et al. [13] proposed FCM_S where the objective function of the classical FCM is modified in order to compensate the intensity in homogeneity and allow the labeling of a pixel to be influenced by the labels in its immediate neighborhood. One disadvantage of FCM_S is that the neighborhood labeling is computed in each iteration step, something that is very time-consuming. Chen and Zhang [16] proposed FCM_S1 and FCM_S2, two variants of FCM_S algorithm in order to reduce the computational time. These two algorithms introduced the extra mean and median-filtered image, respectively, which can be computed in advance, to replace the neighborhood

term of FCM_S. Thus, the execution times of both FCM_S1 and FCM_S2 are considerably reduced.

Afterward, Chen and Zhang [16] improved the FCM_S objective function to more likely reveal inherent non-Euclidean structures in data and more robustness to noise. They then replaced the Euclidean distance by a kernel-induced distance and proposed kernel versions of FCM with spatial constraints, called KFCM_S1 and KFCM_S2. However, the main drawback of FCM_S and its variants FCM_S1 and FCM_S2 and KFCM_S1 and KFCM_S2 is that their parameters heavily affect the final clustering results.

Szilagyi et al. [17] proposed the enhanced FCM (EnFCM) algorithm to accelerate the image segmentation process. The structure of the EnFCM is different from that of FCM_S and its variants. First, a linearly-weighted sum image is formed from both original image and each pixel's local neighborhood average gray level. Then clustering is performed on the basis of the gray level histogram instead of pixels of the summed image. Since, the number of gray levels in an image is generally much smaller than the number of its pixels, the computational time of EnFCM algorithm is reduced, while the quality of the segmented image is comparable to that of FCM_S [17].

Cai et al. [20] proposed the fast generalized FCM algorithm (FGFCM) which incorporates the spatial information, the intensity of the local pixel neighborhood and the number of gray levels in an image. This algorithm forms a nonlinearly-weighted sum image from both original image and its local spatial and gray level neighborhood. The computational time of FGFCM is very small, since clustering is performed on the basis of the gray level histogram. The quality of the segmented image is well enhanced [20].

In this paper, an multi-kernel based FCM (MKFCM) algorithm with spatial information has been proposed using two Gaussian kernels in place of single kernel. Further, the membership values are modified by using their neighbors. The modified membership values are more robust noise images. The effectiveness of the proposed method is tested on four sample MRI brain images under different noise conditions and proved that the proposed algorithm is more robust as compared to FCM family algorithms.

The organization paper is: In section I, a brief review of image segmentation given. A concise review of FCM, KFCM, GKFCM and MKFCM is visualized in section II. The proposed MKFCM with spatial biasing is presented in section III. Further, experimental results and discussions to support the algorithm can be seen in section IV. Conclusions are derived in section V.

2. FUZZY C-MEAN ALGORITHMS (FCM)

2.1 Standard FCM Algorithm

A fuzzy set-theoretic model provides a mechanism to represent and manipulate uncertainty within an image. The concept of fuzzy sets in which imprecise knowledge can be used to define an event. A number of fuzzy approaches for image segmentation are available. Fuzzy C-means is one of the well-known clustering techniques.

Fuzzy c-means clustering algorithm a generalization of the hard c-means algorithm yields extremely good results in image region clustering and object classification. As in hard k-means algorithm, Fuzzy C-means algorithm is based on the minimization of a criterion function.

Suppose a matrix of n data elements (image pixels), each of size $s(s=1)$ is represented as $X = (x_1, x_2, \dots, x_n)$. FCM establishes the clustering by iteratively minimizing the objective function given in Eq. (1).

$$\text{Objective function: } O_m(U, C) = \sum_{i=1}^c \sum_{j=1}^n U_{ij}^m D^2(x_j, C_i) \quad (1)$$

$$\text{Constraint: } \sum_{i=1}^c U_{ij} = 1; \quad \forall j$$

Where, U_{ij} is membership of the j^{th} data in the i^{th} cluster C_i , m is fuzziness of the system ($m=2$) and D is the distance between the cluster center and pixel.

FCM algorithm

Figure 1 shows the flow chart of FCM algorithm and the implementation steps are given below:

Input: Raw image; Output: Segmented image;

- Initialize the cluster centers C_i ($c = 3$ clusters).
- Calculate the distance D between the cluster center and pixel by using eq. (2).

$$D^2(x_j, C_i) = \|x_j - C_i\|^2 \quad (2)$$

- Calculate the membership values by using Eq. (3).

$$U_{ij} = \frac{(D(x_j, C_i))^{-1/(m-1)}}{\sum_{k=1}^c (D(x_j, C_k))^{-1/(m-1)}} \quad (3)$$

- Update the cluster centers using Eq. (4).

$$C_i = \frac{\sum_{j=1}^n U_{ij}^m x_j}{\sum_{j=1}^n U_{ij}^m} \quad (4)$$

- The iterative process starts:
 1. Update the membership values U_{ij} by using Eq. (3).
 2. Update the cluster centers C_i by using Eq. (4).
 3. Update the distance D using Eq. (2).
 4. If $|C_{new} - C_{old}| > \epsilon$; ($\epsilon = 0.001$) then go to step1
 5. Else stop

Assign each pixel to a specific cluster for which the membership is maximal

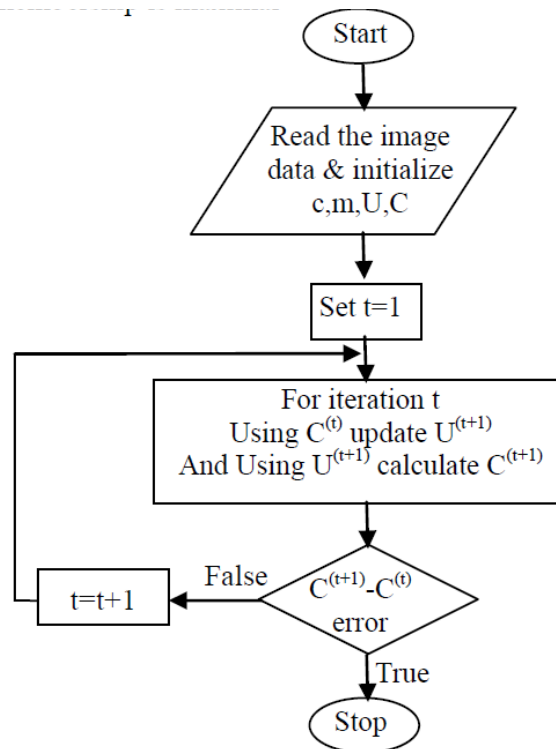


FIGURE 1: Standard FCM Flowchart.

2.2 Kernel Based FCM

Kernel version of the FCM algorithm and its objective function with the mapping as follows:

$$\text{Objective function: } O_m(U, C) = \sum_{i=1}^c \sum_{j=1}^n U_{ij}^m (1 - K(x_j, C_i)) \tag{5}$$

Thus, the update equations for the necessary conditions for minimizing $O_m(U, C)$ are as follows:

$$C_i = \frac{\sum_{j=1}^n U_{ij}^m K(x_j, C_i) x_j}{\sum_{j=1}^n U_{ij}^m K(x_j, C_i)}; \quad i = 1, 2, \dots, C \tag{6}$$

$$U_{ij} = \frac{(1 - K(x_j, C_i))^{-1/(m-1)}}{\sum_{k=1}^c (1 - K(x_j, C_k))^{-1/(m-1)}}; \quad j = 1, 2, \dots, n \tag{7}$$

We point out that the necessary conditions for minimizing $O_m(U, C)$ are update Eqs. (6) and (7) only when the kernel function K is chosen to be the Gaussian function with $K(x_j, C_i) = \exp(-\|x_j - C_i\|^2 / \sigma^2)$. Different kernels can be chosen by replacing the Euclidean distance for different purposes. However, a Gaussian kernel is suitable for clustering in which it can actually induce the necessary conditions. The above proposed KFCM algorithm is very sensitive to the noise. To address this problem Chen and Zhang [16] have proposed the KFCM_S1 and KFCM_S2 algorithms which are utilized the spatial neigh pixel information by introduce α parameter.

2.3 Gaussian Kernal FCM (GKFCM)

It is mentioned that the parameter α is used to control the effect of the neighbors for adjusting the spatial bias correction term. In fact, the parameter α heavily affects the clustering results of KFCM_S1 and KFCM_S2. Intuitively, it would be better if we can adjust each spatial bias correction term separately for each cluster i . That is, the overall parameter α is better replaced with $\hat{\eta}_i$ that is correlated to each cluster i . In this sense, Miin-Shen and Hsu-Shen [21] have considered the following modified objective function $O_m^G(U, C)$ with

$$O_m^G(U, C) = \sum_{i=1}^c \sum_{j=1}^n U_{ij}^m (1 - K(x_j, C_i)) + \sum_{i=1}^c \sum_{j=1}^n \eta_i U_{ij}^m (1 - K(\bar{x}_j, C_i)) \tag{8}$$

where $K(x_j, C_i) = \exp(-\|x_j - C_i\|^2 / \sigma^2)$, \bar{x}_j is the mean of the neighbor pixels, σ^2 is the variance of the total image.

$$C_i = \frac{\sum_{j=1}^n U_{ij}^m (K(x_j, C_i)x_j + \eta_i K(\bar{x}_j, C_i)\bar{x}_j)}{\sum_{j=1}^n U_{ij}^m (K(x_j, C_i) + \eta_i K(\bar{x}_j, C_i))}; i = 1, 2, \dots, C \tag{9}$$

$$U_{ij} = \frac{\left((1 - K(x_j, C_i)) + \eta_i (1 - K(\bar{x}_j, C_i)) \right)^{-1/(m-1)}}{\sum_{k=1}^c \left((1 - K(x_j, C_k)) + \eta_k (1 - K(\bar{x}_j, C_k)) \right)^{-1/(m-1)}}; i = 1, 2, \dots, C; j = 1, 2, \dots, n \tag{10}$$

2.4 Multiple-Kernal Based FCM (MKFCM)

KFCM_S1, KFCM_S2 and GKFCM methods are utilized only one kernel (Gaussian) function but the multiple-kernel methods provide us a great tool to fuse information from different sources [22]. To clarify that, Long et. al [23] used the term “multiple kernel” in a wider sense than the one used in machine learning community. In the machine learning community, “multiple-kernel learning” refers to the learning using an ensemble of basis kernels (usually a linear ensemble), whose combination is optimized in the learning process. The Eq. (11) and (12) are modified as follows.

$$C_i = \frac{\sum_{j=1}^n U_{ij}^m K_M(x_j, C_i)x_j}{\sum_{j=1}^n U_{ij}^m K_M(x_j, C_i)}; i = 1, 2, \dots, C \tag{11}$$

$$U_{ij} = \frac{\left(1 - K_M(x_j, C_i) \right)^{-1/(m-1)}}{\sum_{k=1}^c \left(1 - K_M(x_j, C_k) \right)^{-1/(m-1)}}; i = 1, 2, \dots, C; j = 1, 2, \dots, n \tag{12}$$

Where $K_M(x_j, C_i) = K_1(x_j, C_i) \times K_2(x_j, C_i)$,

$$K_1(x_j, C_i) = \exp(-\|x_j - C_i\|^2 / \sigma_1^2)$$

$$K_2(x_j, C_i) = \exp(-\|x_j - C_i\|^2 / \sigma_2^2).$$

3. MKFCM WITH SPATIAL BIASING

The proposed MKFCM does not consider the spatial neighbor pixel information. Hence, MKFCM is very sensitive for the noise image segmentation. To address the effect of noise in image

segmentation, in this paper, a generalized a novel multiple-kernel fuzzy c-means (FCM) (NMKFCM) methodology with spatial information is introduced. In this paper, NMKFCM is represented as MKFCM_S1 and MKFCM_S2 for reader's clarity (see in Figure 2). The objective function, cluster centers and membership functions for the proposed method are given bellow.

$$O_m^G(U, C) = \sum_{i=1}^c \sum_{j=1}^n U_{ij}^m (1 - K_M(x_j, C_i)) + \sum_{i=1}^c \sum_{j=1}^n \eta_i U_{ij}^m (1 - K_M(\bar{x}_j, C_i)) \quad (13)$$

Where $K_M(x_j, C_i) = K_1(x_j, C_i) \times K_2(x_j, C_i)$,

$$K_1(x_j, C_i) = \exp(-\|x_j - C_i\|^2 / \sigma_1^2),$$

$$K_2(x_j, C_i) = \exp(-\|x_j - C_i\|^2 / \sigma_2^2).$$

\bar{x}_j is the mean for MKFCM_S1 and median for MKFCM_S2 of the neighbor pixels, σ_1^2 , σ_2^2 are the variances.

$$C_i = \frac{\sum_{j=1}^n U_{ij}^m (K_M(x_j, C_i)x_j + \eta_i K_M(\bar{x}_j, C_i)\bar{x}_j)}{\sum_{j=1}^n U_{ij}^m (K_M(x_j, C_i) + \eta_i K_M(\bar{x}_j, C_i))}; \quad i = 1, 2, \dots, C \quad (14)$$

$$U_{ij} = \frac{\left((1 - K_M(x_j, C_i)) + \eta_i (1 - K_M(\bar{x}_j, C_i)) \right)^{-1/(m-1)}}{\sum_{k=1}^c \left((1 - K_M(x_j, C_k)) + \eta_i (1 - K_M(\bar{x}_j, C_k)) \right)^{-1/(m-1)}}; \quad i = 1, 2, \dots, C \quad (15)$$

$$\eta_i = \frac{\min_{i \neq k} (1 - K(C_i, C_k))}{\min_k (1 - K(C_k, x))}; \quad i = 1, 2, \dots, C \quad (16)$$

The proposed method is robust to noise for image segmentation application and the same has been proved from experimental results and discussion in section 4.

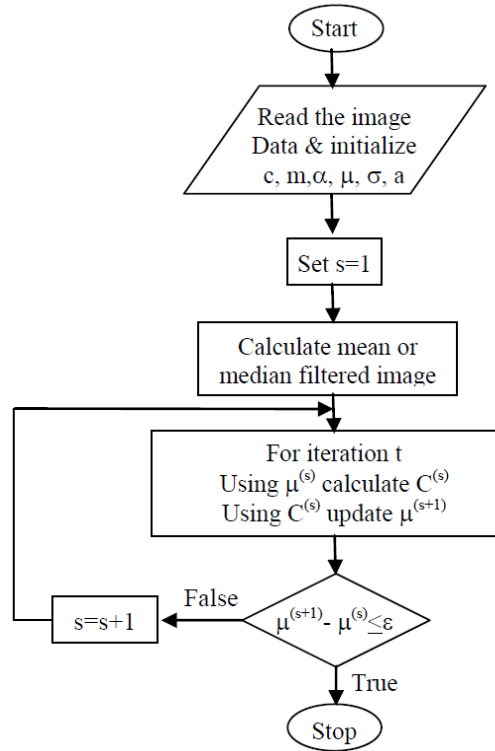


FIGURE 2: Flowchart of MKFCM with spatial biasing.

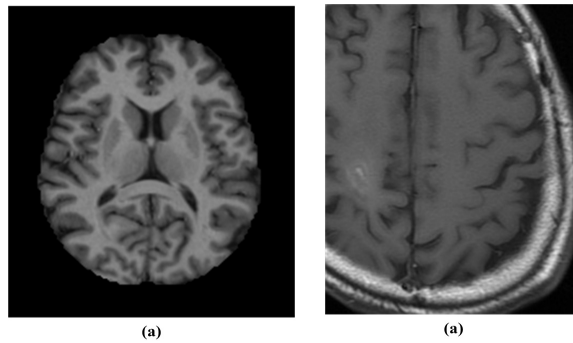


FIGURE 3: Sample images used for experiments

TABLE 1: MRI data acquisition details [26]

| Sequence | MP-RAGE |
|---------------------|----------|
| TR (msec) | 9.7 |
| TE (msec) | 4.0 |
| Flip angle (o) | 10 |
| TI (msec) | 20 |
| TD (msec) | 200 |
| Orientation | Sagittal |
| Thickness, gap (mm) | 1.25, 0 |
| Resolution (pixels) | 176x208 |

4. EXPERIMENTAL RESULTS AND DISCUSSIONS

In order to verify the effectiveness of the proposed algorithm, experiments were conducted on four brain MRIs [24] to compare the performance of the proposed algorithm with other existing methods.

The Open Access Series of Imaging Studies (OASIS) [24] is a series of magnetic resonance imaging (MRI) dataset that is publicly available for study and analysis. This dataset consists of a cross-sectional collection of 421 subjects aged 18 to 96 years. The MRI acquisition details are given in Table 1. The performance of the proposed method is evaluated in terms of score, number of iterations and time. Figure 3 illustrates the sample images selected for experimentation.

4.1. Score Calculation

For comparing segmentation results of different algorithms with a quantitative measure, we use the comparison score defined in [25] and [26]. The comparison score S_{ik} was defined as:

$$S_{ik} = \frac{A_{ik} \cap A_{refk}}{A_{ik} \cup A_{refk}} \quad (17)$$

Where A_{ik} represents the set of pixels belonging to the k^{th} class found by the i^{th} algorithm and A_{refk} represents the set of pixels belonging to the k^{th} class in the reference segmented image.

4.2. Experimental Results with Gaussian Noise

Figure 4 and 6 are the segmentation results obtained with 20% Gaussian noise. In Figure 4, the full size of sample images is used and in Figure 6, the region of interest (ROI) based image segmentation. Tables 2-5 summarize the performance of various methods with different Gaussian and salt & pepper noise. The performance of the proposed methods (MKFCM_S1 and MKFCM_S2) is compared to KFCM_S1, KFCM_S2, GKFCM_S1, GKFCM_S2 and MKFCM. The performance of the methods is evaluated on the basis of score. From Tables 2-5 and Figures 3 and 6, MKFCM_S1 is showing better performance as compared to other existing methods (KFCM, GKFCM and MKFCM) in terms of score.

TABLE 2: Comparison of various technics interms of score on Figure (a) at differnt Gaussian noise
 noise
 Cj: Cluster

| | Gaussian Noise (%) | | | | | | | | | | | |
|-----------------|--------------------|------|------|------|------|------|------|------|------|------|------|------|
| | 5% | | | 10% | | | 15% | | | 20% | | |
| | CI-1 | CI-2 | CI-3 | CI-1 | CI-2 | CI-3 | CI-1 | CI-2 | CI-3 | CI-1 | CI-2 | CI-3 |
| KFCM-S1 | 0.50 | 0.69 | 0.81 | 0.50 | 0.66 | 0.84 | 0.50 | 0.63 | 0.82 | 0.48 | 0.59 | 0.79 |
| KFCM-S2 | 0.45 | 0.66 | 0.86 | 0.47 | 0.62 | 0.83 | 0.45 | 0.58 | 0.80 | 0.44 | 0.55 | 0.77 |
| GKFCM-S1 | 0.42 | 0.60 | 0.83 | 0.41 | 0.53 | 0.77 | 0.44 | 0.49 | 0.73 | 0.42 | 0.46 | 0.71 |
| GKFCM-S2 | 0.40 | 0.59 | 0.82 | 0.41 | 0.51 | 0.76 | 0.41 | 0.47 | 0.72 | 0.41 | 0.44 | 0.69 |
| MKFCM | 0.45 | 0.51 | 0.75 | 0.39 | 0.41 | 0.67 | 0.36 | 0.36 | 0.63 | 0.34 | 0.33 | 0.58 |
| MKFCM-S1 | 0.54 | 0.69 | 0.88 | 0.55 | 0.66 | 0.84 | 0.54 | 0.64 | 0.83 | 0.56 | 0.61 | 0.81 |
| MKFCM-S2 | 0.46 | 0.66 | 0.86 | 0.46 | 0.62 | 0.82 | 0.48 | 0.59 | 0.81 | 0.48 | 0.56 | 0.78 |
| | | | | | | | | | | | | |

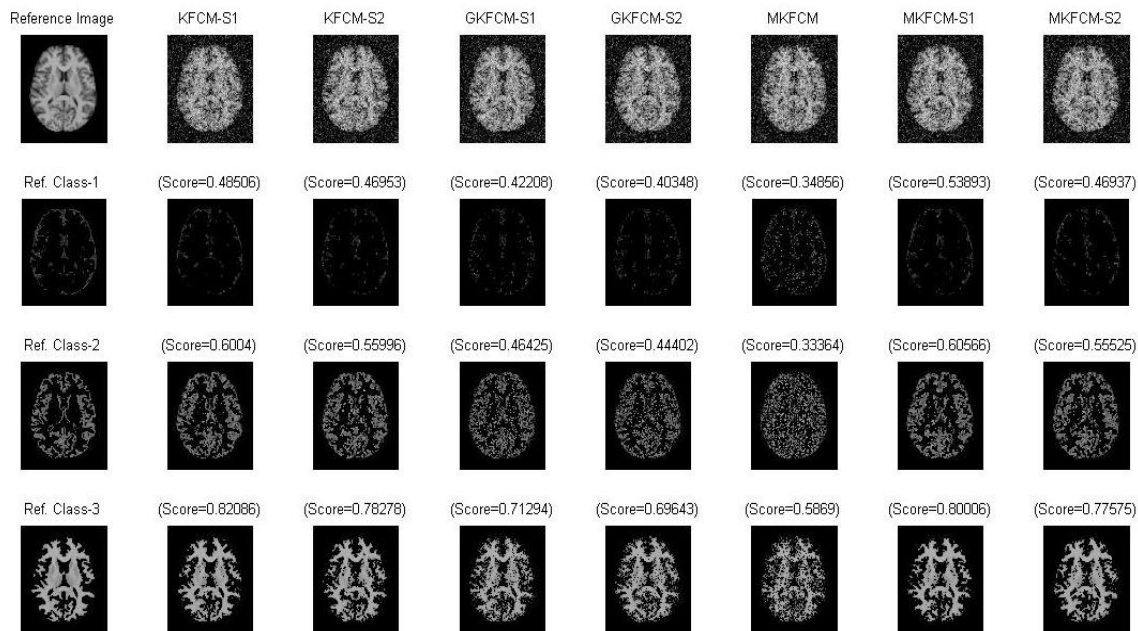


FIGURE 4: Comparison of proposed methods (MKFCM_S1 and MKFCM_S2) with other existing methods (KFCM_S1, KFCM_S2, GKFCM_S1, GKFCM_S2 and MKFCM) in terms of score. The original images are corrupted by Gaussian noise.

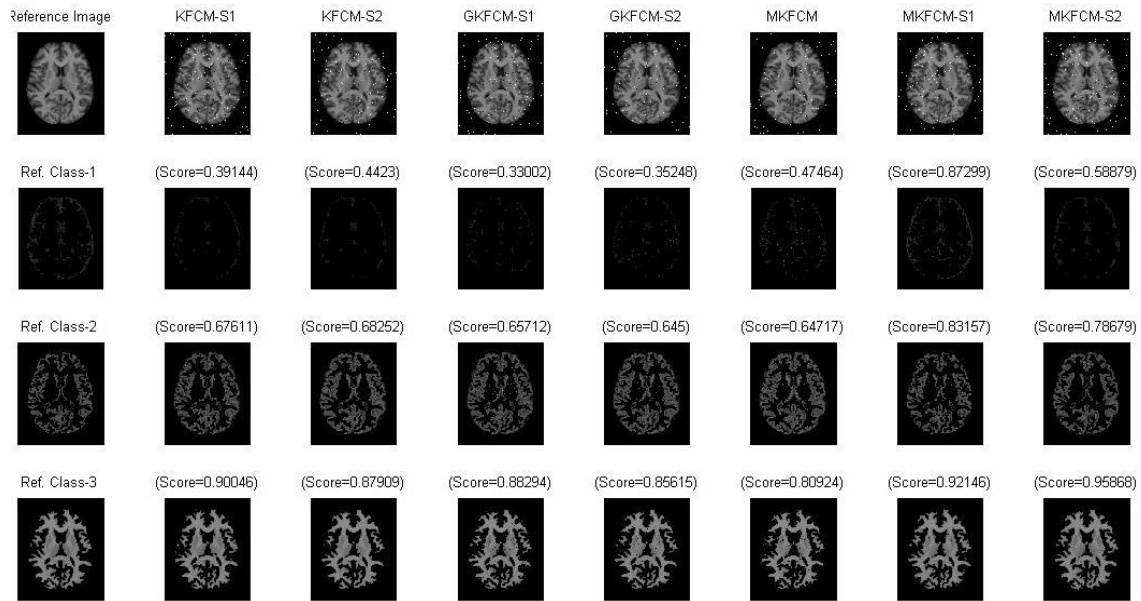


FIGURE 5: Comparison of proposed methods (MKFCM_S1 and MKFCM_S2) with other existing methods (KFCM_S1, KFCM_S2, GKFCM_S1, GKFCM_S2 and MKFCM) in terms of score. The original images are corrupted by salt & Pepper noise.

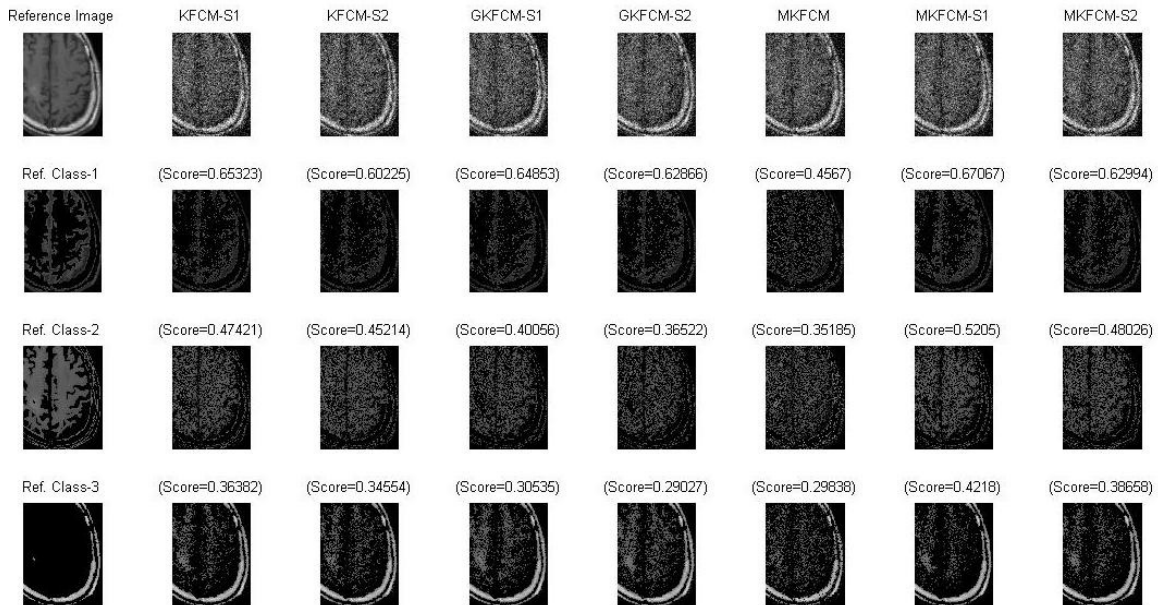


FIGURE 6: Comparison of proposed methods (MKFCM_S1 and MKFCM_S2) with other existing methods (KFCM_S1, KFCM_S2, GKFCM_S1, GKFCM_S2 and MKFCM) in terms of score. The original images are corrupted by Gaussian noise.

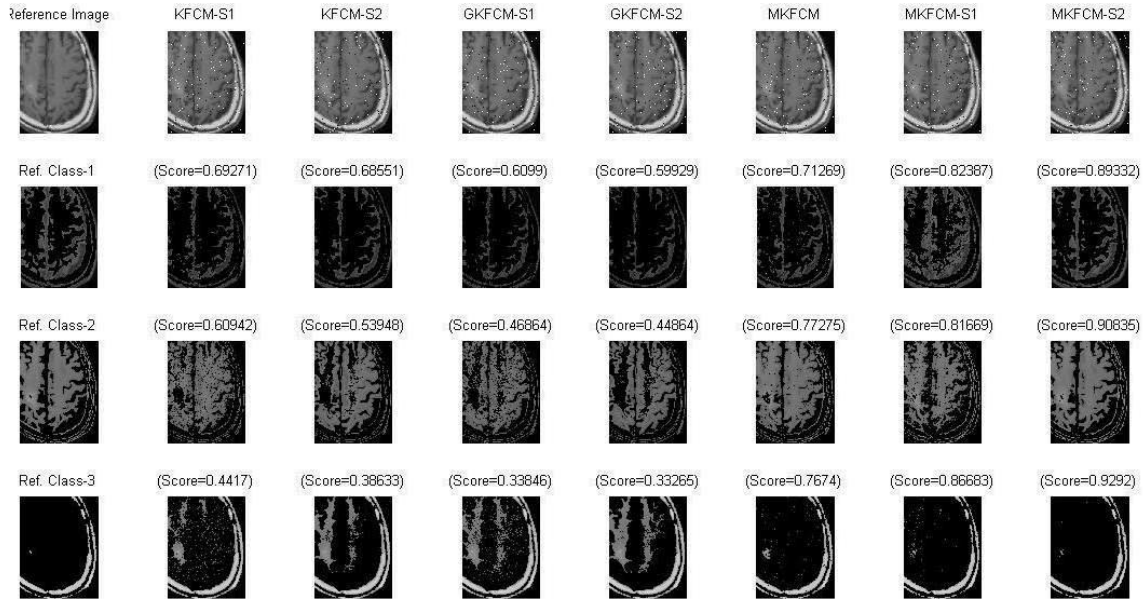


FIGURE 7: Comparison of proposed methods (MKFCM_S1 and MKFCM_S2) with other existing methods (KFCM_S1, KFCM_S2, GKFCM_S1, GKFCM_S2 and MKFCM) in terms of score. The original images are corrupted by salt & pepper noise.

TABLE 3: Comparison of various techniques in terms of score on Figure (b) at different Gaussian noise
C_i: Cluster.

| | Gaussian Noise (%) | | | | | | | | | | | |
|-----------------|--------------------|------|------|------|------|------|------|------|------|------|------|------|
| | 5% | | | 10% | | | 15% | | | 20% | | |
| | CI-1 | CI-2 | CI-3 | CI-1 | CI-2 | CI-3 | CI-1 | CI-2 | CI-3 | CI-1 | CI-2 | CI-3 |
| KFCM-S1 | 0.70 | 0.52 | 0.37 | 0.69 | 0.50 | 0.36 | 0.66 | 0.48 | 0.36 | 0.64 | 0.47 | 0.36 |
| KFCM-S2 | 0.68 | 0.52 | 0.37 | 0.65 | 0.48 | 0.35 | 0.62 | 0.46 | 0.35 | 0.60 | 0.45 | 0.34 |
| GKFCM-S1 | 0.64 | 0.43 | 0.31 | 0.68 | 0.43 | 0.31 | 0.67 | 0.41 | 0.30 | 0.66 | 0.40 | 0.30 |
| GKFCM-S2 | 0.64 | 0.41 | 0.30 | 0.66 | 0.40 | 0.30 | 0.65 | 0.38 | 0.29 | 0.62 | 0.37 | 0.29 |
| MKFCM | 0.58 | 0.45 | 0.36 | 0.51 | 0.39 | 0.33 | 0.47 | 0.36 | 0.30 | 0.45 | 0.35 | 0.29 |
| MKFCM-S1 | 0.79 | 0.67 | 0.51 | 0.73 | 0.60 | 0.46 | 0.70 | 0.55 | 0.43 | 0.67 | 0.52 | 0.42 |
| MKFCM-S2 | 0.77 | 0.68 | 0.47 | 0.70 | 0.55 | 0.42 | 0.66 | 0.50 | 0.40 | 0.64 | 0.47 | 0.38 |

TABLE 4: Comparison of various techniques in terms of score on Figure (a) at different Salt & Pepper Noise
C_i: Cluster.

| | Salt & Pepper Noise (%) | | | | | | | | | | | |
|-----------------|-------------------------|------|------|------|------|------|------|------|------|------|------|------|
| | 5% | | | 10% | | | 15% | | | 20% | | |
| | CI-1 | CI-2 | CI-3 | CI-1 | CI-2 | CI-3 | CI-1 | CI-2 | CI-3 | CI-1 | CI-2 | CI-3 |
| KFCM-S1 | 0.41 | 0.69 | 0.9 | 0.40 | 0.69 | 0.91 | 0.40 | 0.67 | 0.90 | 0.39 | 0.67 | 0.90 |
| KFCM-S2 | 0.44 | 0.68 | 0.88 | 0.44 | 0.68 | 0.88 | 0.44 | 0.68 | 0.88 | 0.44 | 0.68 | 0.87 |
| GKFCM-S1 | 0.34 | 0.67 | 0.89 | 0.33 | 0.66 | 0.88 | 0.31 | 0.66 | 0.88 | 0.33 | 0.65 | 0.88 |
| GKFCM-S2 | 0.35 | 0.66 | 0.88 | 0.35 | 0.65 | 0.87 | 0.35 | 0.65 | 0.86 | 0.35 | 0.64 | 0.85 |
| MKFCM | 0.47 | 0.66 | 0.85 | 0.48 | 0.67 | 0.84 | 0.47 | 0.65 | 0.82 | 0.47 | 0.64 | 0.80 |
| MKFCM-S1 | 0.95 | 0.95 | 0.98 | 0.90 | 0.90 | 0.96 | 0.86 | 0.85 | 0.94 | 0.87 | 0.83 | 0.92 |
| MKFCM-S2 | 0.81 | 0.87 | 0.96 | 0.71 | 0.83 | 0.97 | 0.63 | 0.79 | 0.96 | 0.59 | 0.79 | 0.96 |

TABLE 5: Comparison of various techniques in terms of score on Figure (b) at differnt Salt & Pepper Noise
C_i: Cluster

| | Salt & Pepper Noise (%) | | | | | | | | | | | |
|-----------------|-------------------------|------|------|------|------|------|------|------|------|------|------|------|
| | 5% | | | 10% | | | 15% | | | 20% | | |
| | CI-1 | CI-2 | CI-3 | CI-1 | CI-2 | CI-3 | CI-1 | CI-2 | CI-3 | CI-1 | CI-2 | CI-3 |
| KFCM-S1 | 0.70 | 0.56 | 0.40 | 0.69 | 0.59 | 0.43 | 0.69 | 0.61 | 0.45 | 0.69 | 0.60 | 0.44 |
| KFCM-S2 | 0.68 | 0.53 | 0.38 | 0.68 | 0.51 | 0.36 | 0.68 | 0.51 | 0.36 | 0.68 | 0.53 | 0.38 |
| GKFCM-S1 | 0.59 | 0.42 | 0.31 | 0.59 | 0.43 | 0.31 | 0.60 | 0.44 | 0.32 | 0.60 | 0.46 | 0.33 |
| GKFCM-S2 | 0.58 | 0.42 | 0.31 | 0.59 | 0.43 | 0.32 | 0.59 | 0.44 | 0.32 | 0.59 | 0.44 | 0.33 |
| MKFCM | 0.72 | 0.74 | 0.69 | 0.71 | 0.76 | 0.73 | 0.71 | 0.76 | 0.75 | 0.71 | 0.77 | 0.76 |
| MKFCM-S1 | 0.94 | 0.94 | 0.97 | 0.88 | 0.88 | 0.94 | 0.88 | 0.87 | 0.89 | 0.82 | 0.81 | 0.87 |
| MKFCM-S2 | 0.91 | 0.93 | 0.96 | 0.89 | 0.91 | 0.95 | 0.88 | 0.90 | 0.93 | 0.89 | 0.91 | 0.93 |

4.3. Experimental Results with Salt & Pepper Noise

Figure 5 and 7 are the segmentation results obtained with salt & pepper noise of density 20%. In Figure 5, the full size of sample images is used and in Figure 7, the region of interest (ROI) based image segmentation. The performance of the proposed methods (MKFCM_S1 and MKFCM_S2) is compared to KFCM_S1, KFCM_S2, GKFCM_S1, GKFCM_S2 and MKFCM. The performance of the methods is evaluated on the basis of score. From Figures 5 and 7, MKFCM_S2 is showing better performance as compared to other existing methods (KFCM, GKFCM and MKFCM).

The performance of various methods is also evaluated in terms of number of iterations for convergence of algorithm and time requirement for the algorithm (see in Table 6-9). For time measurement, the evaluation is conducted on Core2Duo computer with speed of 2.66 GHz. From 6-9, it is clear that the proposed methods (MKFCM_S1 and MKFCM_S2) are taking less time as compared to KFCM_S1, KFCM_S2, GKFCM_S1, GKFCM_S2 and MKFCM. Similarly, proposed methods (MKFCM_S1 and MKFCM_S2) are taking less iteration for convergence of the algorithm which are very less as compared to other existing methods, KFCM_S2, GKFCM_S1, GKFCM_S2 and MKFCM. Figure 8 illustrates the comparison of proposed methods with other existing methods. From Figures 4–8, Table 2-9 and above observations, it is clear that the proposed algorithm shows a significant improvement in terms of score, number of iteration and time as compared to other existing methods.

TABLE 6: Comparison of various techniques in terms of number of iterations and execution time at differnt Gaussian noise
NI: Number of iterations; TM: Execution Time (Sec.)

| | Gaussian Noise | | | | | | | |
|-----------------|----------------|------|-----|------|-----|------|-----|------|
| | 5% | | 10% | | 15% | | 20% | |
| | NI | TM | NI | TM | NI | TM | NI | TM |
| KFCM-S1 | 25 | 0.59 | 30 | 0.69 | 24 | 0.56 | 29 | 0.68 |
| KFCM-S2 | 23 | 0.62 | 27 | 0.73 | 30 | 0.83 | 29 | 0.80 |
| GKFCM-S1 | 28 | 0.65 | 30 | 0.68 | 24 | 0.50 | 23 | 0.48 |
| GKFCM-S2 | 22 | 0.57 | 23 | 0.65 | 23 | 0.60 | 30 | 0.81 |
| MKFCM | 35 | 0.96 | 42 | 1.08 | 27 | 0.71 | 28 | 0.69 |
| MKFCM-S1 | 14 | 0.41 | 17 | 0.45 | 22 | 0.54 | 21 | 0.55 |
| MKFCM-S2 | 16 | 0.54 | 20 | 0.64 | 24 | 0.73 | 22 | 0.67 |

TABLE 7: Comparison of various techniques in terms of number of iterations and execution time at differnt Gaussian noise
NI: Number of iterations; TM: Execution Time (Sec.)

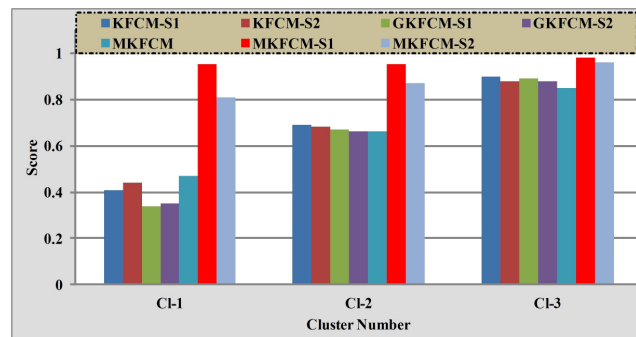
| | Gaussian Noise | | | | | | | |
|-----------------|----------------|-----|-----|-----|-----|-----|-----|-----|
| | 5% | | 10% | | 15% | | 20% | |
| | NI | TM | NI | TM | NI | TM | NI | TM |
| KFCM-S1 | 40 | 2.0 | 44 | 2.3 | 36 | 1.8 | 41 | 2.1 |
| KFCM-S2 | 46 | 2.8 | 31 | 1.8 | 32 | 1.9 | 34 | 2.1 |
| GKFCM-S1 | 35 | 1.7 | 36 | 1.8 | 39 | 2.0 | 32 | 1.6 |
| GKFCM-S2 | 35 | 2.1 | 33 | 2.0 | 32 | 1.8 | 38 | 2.3 |
| MKFCM | 27 | 1.6 | 25 | 1.5 | 28 | 1.6 | 26 | 1.5 |
| MKFCM-S1 | 61 | 3.0 | 42 | 2.2 | 32 | 1.7 | 25 | 1.3 |
| MKFCM-S2 | 50 | 2.9 | 34 | 2.1 | 31 | 1.9 | 27 | 1.7 |

TABLE 8: Comparison of various techniques in terms of number of iterations and execution time at different Salt & Pepper Noise
 NI: Number of iterations; TM: Execution Time (Sec.)

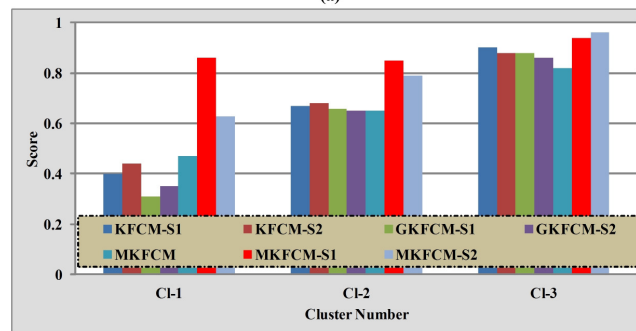
| | Salt & Pepper Noise | | | | | | | |
|-----------------|---------------------|------|-----|------|-----|------|-----|------|
| | 5% | | 10% | | 15% | | 20% | |
| | NI | TM | NI | TM | NI | TM | NI | TM |
| KFCM-S1 | 23 | 0.54 | 28 | 0.62 | 20 | 0.44 | 23 | 0.51 |
| KFCM-S2 | 24 | 0.60 | 23 | 0.58 | 22 | 0.55 | 21 | 0.52 |
| GKFCM-S1 | 18 | 0.36 | 26 | 0.55 | 24 | 0.51 | 26 | 0.56 |
| GKFCM-S2 | 22 | 0.53 | 23 | 0.54 | 25 | 0.61 | 20 | 0.48 |
| MKFCM | 24 | 0.60 | 20 | 0.49 | 21 | 0.51 | 21 | 0.52 |
| MKFCM-S1 | 20 | 0.51 | 19 | 0.49 | 18 | 0.44 | 18 | 0.50 |
| MKFCM-S2 | 27 | 0.75 | 25 | 0.69 | 26 | 0.73 | 19 | 0.58 |

TABLE 9: Comparison of various techniques in terms of number of iterations and execution time at different Salt & Pepper Noise
 NI: Number of iterations; TM: Execution Time (Sec.)

| | Salt & Pepper Noise | | | | | | | |
|-----------------|---------------------|-----|-----|-----|-----|-----|-----|-----|
| | 5% | | 10% | | 15% | | 20% | |
| | NI | TM | NI | TM | NI | TM | NI | TM |
| KFCM-S1 | 61 | 3.2 | 58 | 3.0 | 52 | 2.8 | 51 | 2.7 |
| KFCM-S2 | 78 | 5.0 | 46 | 2.8 | 76 | 4.8 | 53 | 3.3 |
| GKFCM-S1 | 42 | 2.1 | 38 | 1.9 | 62 | 3.3 | 64 | 3.3 |
| GKFCM-S2 | 69 | 4.3 | 43 | 2.6 | 43 | 2.7 | 88 | 5.5 |
| MKFCM | 139 | 9.4 | 80 | 5.2 | 83 | 5.4 | 45 | 2.8 |
| MKFCM-S1 | 47 | 2.4 | 45 | 2.3 | 31 | 1.7 | 43 | 2.2 |
| MKFCM-S2 | 33 | 2.0 | 33 | 2.0 | 31 | 1.9 | 23 | 1.5 |



(a)



(b)

FIGURE 8: Comparison of proposed methods with other existing methods with Salt & Pepper noise: (a) 5% and (b) 15%.

5. CONCLUSIONS

In this paper, new image segmentation algorithms (MKFCM_S1 and MKFCM_S2) which are increasing the performance and decreasing the computational complexity. The algorithm utilizes the spatial neighborhood membership values in the standard kernels are used in the kernel FCM (KFCM) algorithm and modifies the membership weighting of each cluster. The proposed algorithm is applied on brain MRI which degraded by Gaussian noise and Salt-Pepper noise demonstrates that the proposed algorithm performs more robust to noise than other existing image segmentation algorithms from FCM family.

6. REFERENCES

- [1]. X. Munoz, J. Freixenet, X. Cufi, and J. Marti, "Strategies for image segmentation combining region and boundary information," *Pattern Recognition Letters*, vol. 24, no. 1, pp. 375–392, 2003.
- [2]. D. Pham, C. Xu, and J. Prince, "A survey of current methods in medical image segmentation," In *Annual Review of Biomedical Engineering*, vol. 2, pp. 315–337, 2000.
- [3]. Mohammad Ali Balafar, Abd.Rahman Ramli, M.Iqbal Saripan, Syamsiah Mashohor, "Medical Image Segmentation Using Fuzzy C-Mean (Fcm), Bayesian Method And User Interaction," *Proceedings of the 2008 International Conference on Wavelet Analysis and Pattern Recognition*, pp. 68-73, Aug. 2008.
- [4]. László Szilágyi, Sándor M. Szilágyi, Balázs Benyó and Zoltán Benyó, "Application of Hybrid c-Means Clustering Models in Inhomogeneity Compensation and MR Brain Image Segmentation," *5th International Symposium on Applied Computational Intelligence and Informatics*, pp.105-110, May. 2009.
- [5]. MacQueen,J.B. "Some Methods for classification and Analysis of Multivariate Observations,"*Proceedings of 5th Berkeley Symposium on Mathematical Statistics and Probability*. University of California Press, pp. 281–297, 1967.
- [6]. Arthur D,Vassilvitskii S,"How Slow is the k-means Method?," *Proceedings of the 2006 Symposium on Computational Geometry* , June. 2006.
- [7]. L. Zadeh, "Fuzzy sets," *Inf. Control*, vol. 8, pp. 338–353, 1965.
- [8]. J. Udupa and S. Samarasekera, "Fuzzy connectedness and object definition: Theory, algorithm and applications in image segmentation," *Graphical Models and Image Processing*, vol. 58, no. 3, pp. 246–261, 1996.
- [9]. Y. Tolias and S. Panas, "Image segmentation by a fuzzy clustering algorithm using adaptive spatially constrained membership functions," *IEEE Transactions on Systems, Man, and Cybernetics*, vol. 28, no. 3, pp. 359–369, Mar.1998.
- [10]. J. Noordam, W. van den Broek, and L. Buydens, "Geometrically guided fuzzy C-means clustering for multivariate image segmentation," in *Proceedings of the International Conference on Pattern Recognition*, 2000, vol. 1, pp.462–465.
- [11]. M. Yang, Y. J. Hu, K. Lin, and C. C. Lin, "Segmentation techniques for tissue differentiation in MRI of ophthalmology using fuzzy clustering algorithms," *Magnetic Resonance Imaging*, vol. 20, no. 2, pp. 173–179, 2002.
- [12]. G. Karmakar and L. Dooley, "A generic fuzzy rule based image segmentation algorithm," *Pattern Recognition Letters.*, vol. 23, no. 10, pp.1215–1227, 2002.
- [13]. M. Ahmed, S. Yamany, N. Mohamed, A. Farag, and T. Moriarty, "A modified fuzzy C-means algorithm for bias field estimation and segmentation of MRI data," *IEEE Transactions on Medical Imaging*, vol. 21, no. 3, pp. 193–199, 2002.
- [14]. J. Bezdek, "Pattern Recognition with Fuzzy Objective Function Algorithms," *Kluwer Academic Publishers, New York: Plenum*, 1981.

- [15]. D. Pham, "An adaptive fuzzy C-means algorithm for image segmentation in the presence of intensity inhomogeneities," *Pattern Recognition Letters*, vol. 20, pp. 57–68, 1999.
- [16]. S. Chen and D. Zhang, "Robust image segmentation using FCM with spatial constraints based on new kernel-induced distance measure," *IEEE Transactions on Systems, Man, and Cybernetics*, vol. 34, pp. 1907–1916, 2004.
- [17]. L. Szilagyi, Z. Benyo, S. Szilagyii, and H. Adam, "MR brain image segmentation using an enhanced fuzzy C-means algorithm," in *Proceedings of the 25th Annual International Conference of the IEEE EMBS*, pp. 17–21, 2003.
- [18]. M. Krinidis and I. Pitas, "Color texture segmentation based-on the modal energy of deformable surfaces," *IEEE Transactions on Image Processing*, vol. 18, no. 7, pp. 1613–1622, Jul. 2009.
- [19]. D. Pham, "Fuzzy clustering with spatial constraints," in *Proceedings of International Conference on Image Processing*, New York, 2002, vol. II, pp. 65–68.
- [20]. W. Cai, S. Chen, and D. Zhang, "Fast and robust fuzzy c-means clustering algorithms incorporating local information for image segmentation," *Pattern Recognition*, vol. 40, no. 3, pp. 825–838, Mar. 2007.
- [21]. Miin-Shen Yang, Hsu-Shen Tsai, "A Gaussian kernel-based fuzzy c-means algorithm with a spatial bias correction," *Pattern Recognition Letters*, vol. 29, pp. 1713–1725, May 2008.
- [22]. G. Camps-Valls, L. Gomez-Chova, J. Munoz-Mari, J. L. Rojo-Alvarez, and M. Martinez-Ramon, "Kernel-based framework for multitemporal and multisource remote sensing data classification and change detection," *IEEE Trans. Geosci. Remote Sens.*, vol. 46, no. 6, pp. 1822–1835, Jun. 2008.
- [23]. Long Chen, C. L. Philip Chen, and Mingzhu Lu, "A Multiple-Kernel Fuzzy C-Means Algorithm for Image Segmentation," *IEEE Trans. Systems, Man, And Cybernetics—Part B: Cybernetics*, vol. 41, No. 5, pp. 1263 – 1274, February 9,2011.
- [24]. D. S.Marcus, T. H. Wang, J. Parker, J. G. Csernansky, J. C.Morris, and R. L. Buckner, Open access series of imaging studies (OASIS): Crosssectional MRI data in young, middle aged, nondemented, and demented older adults. *J. Cogn. Neurosci.*, 19 (9) 1498–1507, 2007.
- [25]. Masulli, F., Schenone, A., 1999. A fuzzy clustering based segmentation system as support to diagnosis in medical imaging. *Artif. Intell. Med.* 16, 129–147.
- [26].Zhang, D.Q., Chen, S.C., 2004. A novel kernelized fuzzy c-means algorithm with application in medical image segmentation. *Artif. Intell. Med.* 32, 37–50.